Enhanced field emission properties from well-aligned zinc oxide nanoneedles grown on the Au/Ti/*n*-Si substrate

Chan Jun Park and Duck-Kyun Choi
Division of Materials Science and Engineering, Hanyang University, 17 Haengdang-dong, Seongdong-ku, Seoul 133-791, Korea

Jinkyoung Yoo and Gyu-Chul Yi
National CRI Center for Semiconductor Nanorods and Department of Materials Science and Engineering, POSTECH, Pohang, Gyeongbuk 790-784, Korea

Cheol Jin Lee[a)]
School of Electrical Engineering, Korea University, Seoul 136-701, Korea

(Received 12 June 2006; accepted 16 January 2007; published online 22 February 2007)

The authors investigated the field emission from vertically well-aligned zinc oxide (ZnO) nanoneedles grown on the Au/Ti/*n*-Si (100) substrate using metal organic chemical vapor deposition. The turn-on field of ZnO nanoneedles was about 0.85 V/μm at the current density of 0.1 μA/cm^2, and the emission current density of 1 mA/cm^2 was achieved at the applied electric field of 5.0 V/μm. The low turn-on field of the ZnO nanoneedles was attributed to very sharp tip morphology, and the high emission current density was mainly caused by the formation of the stable Ohmic contact between the ZnO nanoneedles and Au film. © *2007 American Institute of Physics*. [DOI: 10.1063/1.2643979]

One-dimensional zinc oxide (ZnO) nanostructures are of particular interest for various device applications due to their unique electrical and optical properties.[1–3] Especially, ZnO nanowires or nanoneedles have attracted much attention as a field emitter because of their high aspect ratio, high mechanical stability, and negative electron affinity.[4–6] There have been some reports on field emission properties from the ZnO nanostructures such as nanowires and nanoneedles.[7–12] The previous reports mainly focused on field emission properties dependent on the shape or the aspect ratio of ZnO nanostructure materials. However, besides above two parameters, the contact property between the ZnO nanostructures and substrates is also an important parameter determining the field emission properties. It is considered that moderate substrate materials may induce the formation of the good Ohmic contact between the ZnO nanostructures and the substrates. But, until now, many reports largely discussed field emission properties from the ZnO nanostructures without consideration of the contact behavior. Recently, we have studied the contact effect on the field emission properties of various nanostructure materials to understand emission performance more exactly.

Here we demonstrated the field emission properties from the ZnO nanoneedles grown on the Au/Ti/*n*-Si (100) substrate using metal organic chemical vapor deposition (MOCVD). We investigated how the substrate materials affect field emission performance of the ZnO nanoneedles. To synthesize the ZnO nanoneedles using MOCVD, diethylzinc and oxygen were used as the reactants and their flow rates were in the ranges of 20–100 and 5–10 SCCM (SCCM denotes cubic centimeter per minute at STP), respectively. Typical growth temperature and the growth time were 500 °C and 2 h, respectively. In this work, we used the Au/Ti/*n*-Si (100) substrate. To fabricate the Au/Ti/*n*-Si (100) substrate, we cleaned the Si substrate in an ultrasonic bath with acetone and methanol. The Ti and Au films were deposited by an electron beam evaporation method. At first, Ti film (50 nm) was deposited on the Si substrate and then Au film (50 nm) was deposited on the Ti deposited Si substrate. Here, the Ti film was used to enhance mechanical adhesion between the Si substrate and the Au film. The ZnO nanoneedles then were synthesized on the Au/Ti/*n*-Si (100) substrate. The as-grown ZnO nanoneedles were characterized by scanning electron microscopy (SEM) (Hitachi S-4700), x-ray diffraction (XRD) (Rigaku DMAX PSPC MDG 2000), and transmission electron microscopy (TEM) (Philips TECNAI UT-30). Field emission properties were measured using a diode structure configuration. The *n*-type Si (100) substrate was used as a cathode and the designed stainless steel rod was used as an anode. Measurement was conducted in a vacuum chamber at a pressure of 1×10^{-6} torr. The distance between the anode and the tip of ZnO nanoneedle was about 300 μm and the measured emission area was 7 mm^2. Emission current was monitored with a Keithley 6517A. Before measuring the field emission current, we performed an electrical annealing to get a uniform field emission property, as reported before. We measured the field emission properties five times at the same position in order to obtain reliable field emission results.

Figure 1 shows SEM images of the well-aligned ZnO nanoneedles grown on the Au/Ti/*n*-Si (100) substrate using MOCVD. As shown in Figs. 1(a) and 1(b), the ZnO nanoneedles have cone-shaped tips and have the diameters of 60–70 nm and the lengths of 0.9–1.0 μm, respectively. Figures 1(c) and 1(d) show SEM images of the top view of the ZnO nanoneedles, which is not vertical in direction but a little tilted direction. They also indicate that the density of the ZnO nanoneedles is about 1.2×10^6/cm^2.

The crystal structure of the ZnO nanoneedles was investigated by XRD. Figure 2 indicates that XRD shows two peaks at 34.42° and 72.59° which correspond to ZnO(0002)

a)Author to whom correspondence should be addressed; electronic mail: cjlee@korea.ac.kr

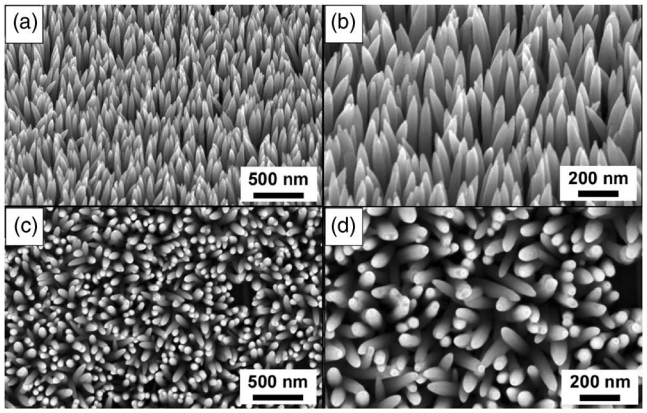

FIG. 1. SEM images of the ZnO nanoneedles grown on the Au/Ti/*n*-Si(100) substrate. (a) The SEM image of the ZnO nanoneedles which have cone-shaped tips and the diameters of 60–70 nm. (b) The magnified SEM image of the ZnO nanoneedles. (c) Top view of the ZnO nanoneedles, which is not vertical in direction but a little tilted direction, and have the density of about $1.2\times10^6/\mathrm{cm}^2$. (d) The magnified SEM image of top view of the ZnO nanoneedles.

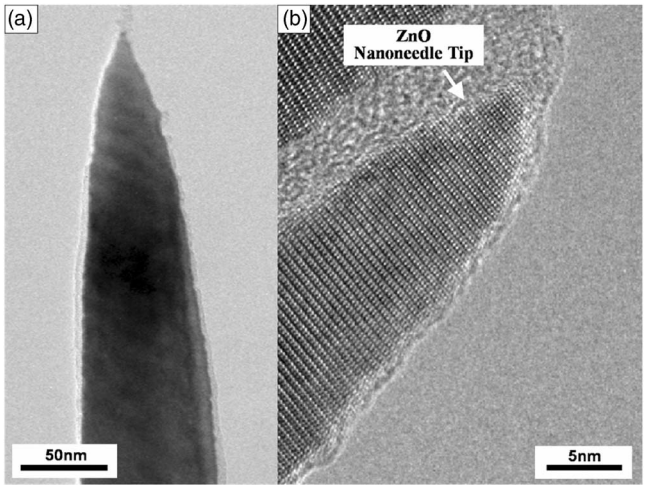

FIG. 3. TEM images of a ZnO nanoneedle grown on the Au/Ti/*n*-Si(100) substrate. (a) The TEM image of the ZnO nanoneedle with a sharp-curvature tip. (b) The HRTEM image of the ZnO nanoneedle exhibiting lattice fringes clearly observed.

and ZnO(0004), respectively. This result indicates that the ZnO nanoneedles exhibit their *c* axis normal to the substrate and a wurtzite structure. From XRD analysis, besides of ZnO(0002) and ZnO(0004) peaks, we can see several different peaks at 68.85°, 69.11°, and 69.32°, which indicate the formation of alloy materials corresponding to $AuTi_3(321)$, $Au_3Zn(003)$, and $Au_3Zn(035)$, respectively.

Figure 3 shows TEM images of a ZnO nanoneedle grown on the Au/Ti/*n*-Si (100) substrate. Figure 3(a) exhibits the ZnO nanoneedle which has a sharp-curvature tip. The diameter of ZnO nanoneedle is about 70 nm at the bottom but decreases toward the tip, resulting in the corn shape. In Fig. 3(b), the high resolution TEM (HRTEM) image indicates that the ZnO nanoneedle follows *c* axis growth direction, and has rare dislocations and stacking faults, which reveals high crystalline single crystal structure.

The field emission properties from the ZnO nanoneedles grown on the Au/Ti/*n*-Si substrate were measured, as shown in Fig. 4. The ZnO nanoneedles show the low turn-on field of about 0.85 V/μm at the current density of 0.1 μA/cm^2 and the high emission current density of about 1 mA/cm^2 at the applied electric field of 5.0 V/μm. It is considered that the ZnO nanoneedles indicate much higher emission performance compared with other ZnO nanoneedles or ZnO nanowires.[7–15] In our previous work, the ZnO nanowires directly grown on Si substrate showed the turn-on field of about 6.0 V/μm at current density of 0.1 μA/cm^2 and the emission current density about 1 mA/cm^2 at the applied electric field of 11.0 V/μm.[8] The needlelike ZnO nanowires grown on the Ga-doped $ZnO/Si_3N_4/SiO_2/Si$ substrate showed the turn-on field of about 20 V/μm at the current density of 0.1 μA/cm^2 and the current density of about 0.1 mA/cm^2 at a bias field of 30 V/μm.[9] The well-aligned ZnO nanowires grown on Si subsrate showed the emission current density of 1 mA/cm^2 at the bias field of 6.5 or 8.3 V/μm.[10,11] Cao *et al.*[13] showed that the turn-on field of the ZnO nanoneedles grown on Au/Si substrate using electrochemical deposition route was about 4 V/μm at the current density of 0.1 μA/cm^2 and the emission current density was 10 μA/cm^2 at a bias field of 18.9 V/μm. Yang *et al.*[15] reported that the turn-on field of the pencil-like ZnO nanowires grown on amorphous carbon was about 3.7 V/μm at

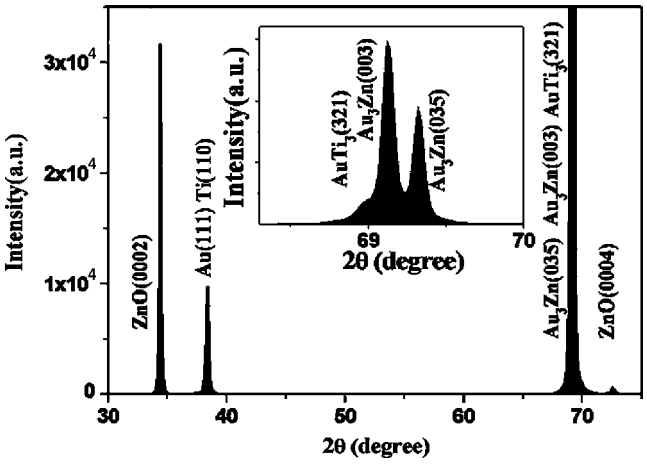

FIG. 2. XRD pattern of the ZnO nanoneedles grown on the Au/Ti/*n*-Si(100) substrate. It shows several peaks at 34.42°, 38.18°, 38.48°, 68.85°, 69.11°, 69.32°, and 72.59° corresponding to ZnO(0002), Au(111), Ti(110), $AuTi_3(321)$, $Au_3Zn(003)$, $Au_3Zn(035)$, and ZnO(0004), respectively. The inset shows a magnified image of the peaks between 68° and 70°.

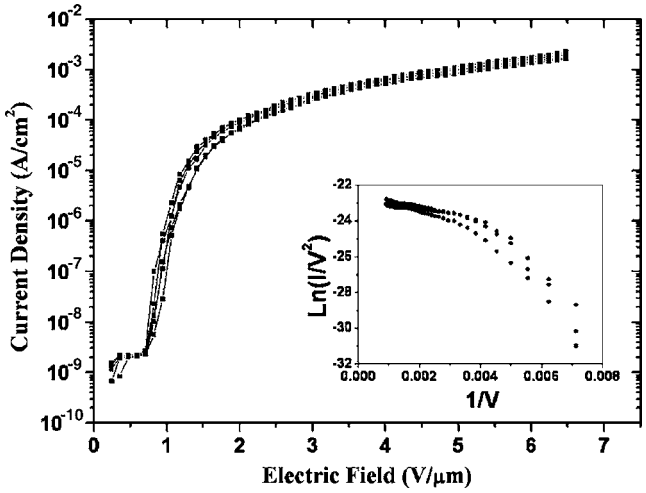

FIG. 4. Field emission properties of the ZnO nanoneedles grown on the Au/Ti/*n*-Si substrate. The inset shows the FN plots.

the current density of 0.1 $\mu A/cm^2$ and the emission current density was 1 mA/cm^2 over the electric field of 8.0 $V/\mu m$. However, interestingly, Ren and co-workers obtained very high emission current from ZnO nanowires grown on carbon cloth or vertically aligned ultralong ZnO nanobelts.[16–18] According to their reports, the ZnO nanowire showed the emission current density of about 1 mA/cm^2 at the applied electric field of about 0.7 $V/\mu m$, while the vertically aligned ultralong ZnO nanobelts indicated the emission current density of about 1 mA/cm^2 at the applied electric field of about 1.3 $V/\mu m$. It is considered that such high emission current was attributed to high field enhancement factor due to a unique morphology of the ZnO nanostructures. In order to compare the field emission properties of ZnO nanoneedles dependent on the substrate, we evaluated the field emission properties of ZnO nanoneedles grown on the *n*-Si (100) substrate using MOCVD. In our experimental result, the turn-on field of the ZnO nanoneedles was about 7.0 $V/\mu m$ at the current density of 0.1 $\mu A/cm^2$ and the emission current density was about 0.3 mA/cm^2 at the applied electric field of about 18 $V/\mu m$. On the other hand, our ZnO nanoneedles grown on Au/Ti/*n*-Si substrate indicated much higher emission performance compared with the previous results. Moreover, our ZnO nanoneedles grown on Au/Ti/*n*-Si substrate showed the stable emission behavior without fluctuation during an emission measurement. It was well known that Schottky contact could easily be formed between ZnO materials and Au film after the moderate post-treatment.[19–21] In this work, we consider that the Ohmic contact might be formed between the ZnO nanoneedles and the Au film because the growth temperature of ZnO nanoneedles was about 500 °C. In general, the reaction temperature is so high that the spontaneous alloy formation between Au and Zn can appear, resulting in stable Ohmic contacts with a low specific contact resistance.[22,23] From XRD data, we could find the Au_3Zn alloy peaks such as $Au_3Zn(003)$ and $Au_3Zn(035)$, which can promise the Ohmic contact between the ZnO nanoneedles and the Au film.[24] As a result, the ZnO nanoneedles grown on the Au/Ti/*n*-S1 substrate can achieve the enhanced field emission performance.

The Fowler-Nordheim (FN) plot is shown in the inset of Fig. 4. It exhibits two linear behaviors in the measurement range. Emission current-voltage characteristics can be analyzed by FN equation for the field emission,

$$J = A\left(\frac{\beta^2 V^2}{\Phi d^2}\right)\exp\left(-\frac{B\Phi^{3/2} d}{\beta V}\right),$$

where J is the current density, $A = 1.56 \times 10^{-6}$ ($A\ V^{-2} eV$), $B = 6.83 \times 10^9$ ($V\ eV^{-3/2}\ V\ m^{-1}$), β is a field enhancement factor, Φ is the work function, $E = (V/d)$ is the applied field, d is a distance between the anode and the cathode, and V is the applied voltage.[8] Here, the field enhancement factor (β) can be calculated from the slope of FN plot if the work function of the emitter is known. The measured value of the work function of ZnO nanoneedles was about 5.3 eV.[25] The field enhancement factor (β) of ZnO nanoneedles grown on the Au/Ti/*n*-Si substrate is about 8328. We consider that the high field enhancement factor (β) of ZnO nanoneedles is manly caused by a unique morphology of the ZnO nanoneedles, showing a very sharp curvature at the tip, as shown in Fig. 1.

In summary, we demonstrate the high field emission properties from the cone-shaped ZnO nanoneedles grown on the Au/Ti/*n*-Si substrate. The low turn-on field of the ZnO nanoneedles was attributed to very sharp tip morphology and the high emission current density was mainly caused by the formation of stable Ohmic contact between the ZnO nanoneedles and the Au film. We emphasize that the stable Ohmic contact is an important parameter to determine field emission property for ZnO nanostructures. It is suggested that the ZnO nanoneedles grown on Au/Ti/*n*-Si substrate can be applied to various field emission devices such as future electron devices flat lamps, x-ray sources, and high-efficient cold cathodes.

This work was supported by the SRC program of Center for Nanotubes and Nanosructured Composites of MOST/KOSEF, by the National R&D Project for Nano Science and Technology, and by the Ministry of Commerce, Industry, and Energy of Korea through a Components and Materials Technology Development project (No.0401-DD2-0162).

[1] D. M. Bagnall, Y. F. Chen, Z. Zhu, T. Yao, S. Koyama, M. Y. Shen, and T. Goto, Appl. Phys. Lett. **70**, 2230 (1997).
[2] M. H. Huang, S. Mao, H. Feik, H. Yan, Y. Wu, H. Kind, E. Weber, R. Russo, and P. Yang, Science **292**, 1897 (2001).
[3] C. H. Liu, W. C. Yiu, F. C. K. Au, J. X. Ding, C. S. Lee, and S. T. Lee, Appl. Phys. Lett. **83**, 3168 (2003).
[4] W. I. Park, G.-C. Yi, M. Kim, and S. J. Pennycook, Adv. Mater. (Weinheim, Ger.) **14**, 1841 (2002).
[5] C. J. Lee, T. J. Lee, S. C. Lyu, Y. Zhang, H. Ruh, H. J. Lee, H. W. Shim, E.-K. Suh, and C. J. Lee, Chem. Phys. Lett. **363**, 134 (2002).
[6] P. X. Gao, Y. Ding, and Z. L. Wang, Nano Lett. **3**, 1315 (2003).
[7] T. Sugino, T. Hori, C. Kimura, and T. Yamamoto, Appl. Phys. Lett. **78**, 3229 (2001).
[8] C. J. Lee, T. J. Lee, S. C. Lyu, Y. Zhang, H. Ruh, and H. J. Lee, Appl. Phys. Lett. **81**, 3648 (2002).
[9] Y. K. Tseng, C. J. Huang, H. M. Cheng, I. N. Lin, K. S. Liu, and I. C. Chen, Adv. Funct. Mater. **13**, 811 (2003).
[10] Y. W. Zhu, H. Z. Zhang, X. C. Sun, S. Q. Feng, J. Xu, Q. Zhao, B. Xiang, B. R. M. Wang, and D. P. Yu, Appl. Phys. Lett. **83**, 144 (2003).
[11] S. H. Jo, J. Y. Lao, Z. F. Ren, R. A. Farrer, T. Baldacchini, and J. T. Fourkas, Appl. Phys. Lett. **83**, 4821 (2003).
[12] H. Z. Zhang, R. M. Wang, and Y. W. Zhu, J. Appl. Phys. **96**, 624 (2004).
[13] B. Q. Cao, W. P. Cai, G. T. Duan, Y. Li, Q. Zhao, and D. P. Yu, Nanotechnology **16**, 2567 (2005).
[14] H. Ham, G. Shen, J. H. Cho, T. J. Lee, S. H. Seo, and C. J. Lee, Chem. Phys. Lett. **404**, 69 (2005).
[15] Y. H. Yang, B. Wang, N. S. Xu, and W. Yang, Appl. Phys. Lett. **89**, 043108 (2006).
[16] S. H. Jo, D. Banerjee, and Z. F. Ren, Appl. Phys. Lett. **85**, 1407 (2004).
[17] D. Banerjee, S. H. Jo, and Z. F. Ren, Adv. Mater. (Weinheim, Ger.) **16**, 2028 (2004).
[18] W. Wang, B. Zeng, J. Yang, B. Poudel, J. Huang, M. J. Naughton, and Z. F. Ren, Adv. Mater. (Weinheim, Ger.) **18**, 3275 (2006).
[19] H. K. Kim, S. H. Han, T. Y. Seong, and W. K. Choi, Appl. Phys. Lett. **77**, 1647 (2000).
[20] W. I. Park, G.-C. Yi, J.-W. Kim, and S. M. Park, Appl. Phys. Lett. **82**, 4358 (2003).
[21] H. L. Mosbacker, Y. M. Strzhemechny, B. D. White, P. E. Smith, D. C. Look, D. C. Reynolds, C. W. Litton, and L. J. Brillson, Appl. Phys. Lett. **87**, 012102 (2005).
[22] H. Yasuda and H. Mori, Phys. Rev. Lett. **69**, 3747 (1992).
[23] C. Borchers, S. Muler, D. Stichtenoth, D. Schwen, and C. Ronning, J. Phys. Chem. B **110**, 1656 (2006).
[24] O. Oparaku, C. L. Dargan, N. M. Pearsall, and R. Hill, Semicond. Sci. Technol. **5**, 65 (1990).
[25] T. Minami, T. Miyata, and T. Yamamoto, Surf. Coat. Technol. **108**, 583 (1998).